

An Interpretation of Small-Ion Effects on the Electrostatics of the λ Repressor DNA Complex

Nancy L. Marky and Gerald S. Manning*

Contribution from the Department of Chemistry, Rutgers University, 610 Taylor Road, Piscataway, New Jersey 08854-8087

Received December 6, 1999. Revised Manuscript Received April 21, 2000

Abstract: Monte Carlo simulations of the interactions of Na^+ and Cl^- ions with λ repressor protein and its DNA operator site have revealed an interesting effect [Jayaram, B.; DiCapua, F. M.; Beveridge, D. L. *J. Am. Chem. Soc.* **1991**, *113*, 5211–5215]. When the protein is close to its binding site on DNA, the presence of the small ions strengthens the electrostatic net attractive force between the formally charged protein residues and the phosphate groups on DNA. The effect has been interpreted as a manifestation of the release of counterions condensed on DNA. We show that although counterions are indeed released, the enhancement of the attractive force at short distances has a different origin. There is a direct attraction between DNA phosphates and positively charged protein residues, and a direct repulsion between DNA phosphates and negatively charged protein residues. Close to the DNA, the net direct force is attractive. By weakening the direct repulsion between DNA phosphates and the negatively charged glutamate and aspartate residues on the protein, the presence of small ions increases the net attraction. A complete understanding of protein–DNA electrostatics thus involves consideration of the interaction of DNA phosphates with anionic as well as cationic protein residues. As a side result of our calculations, we estimate the effect of small ions on the binding free energy of the repressor–operator complex (from the isolated species) as unfavorable at about 40–45 kcal/mol.

1. Introduction

Our intuitive expectations of the effect of small ions on electrostatic interactions have largely been molded by the screening theory of Debye and Hückel. The distance dependence of the attractive potential between a Na^+ cation and a Cl^- anion in NaCl solution has the limiting form $-\exp(-\kappa r)/r$, where the effect of the other Na^+ and Cl^- ions is incorporated into the screening parameter κ , proportional to the square root of NaCl concentration. If we subtract the direct Coulomb potential $-1/r$ from the screened potential to isolate the effect of salt, we get the function $[1 - \exp(-\kappa r)]/r$, which is positive for all separation distances r . Thus, the effect of the other Na^+ and Cl^- ions on the direct attractive interaction between a given Na^+ and Cl^- pair is to add an unfavorable free energy to it, effectively decreasing the attraction.

Jayaram, DiCapua, and Beveridge¹ have performed a Monte Carlo (MC) free energy simulation of a protein–DNA complex that isolates the effect of small ions on the interaction. The λ repressor is a transcription regulatory protein that binds to a specific promoter sequence of DNA base pairs, the operator site. There are many positively charged (lysine, arginine) and negatively charged (glutamate, aspartate) residues on the protein, but there is an excess of positive protein charge at the interface of the complex, and the salt concentration dependence of the association constant for the complex is about the same as that for the binding of a divalent or trivalent cation (positive charge) to the polyanionic field of DNA. A reasonable expectation is that the direct electrostatic attraction between protein and DNA would be weakened by the screening effect of the Na^+ and Cl^- ions present in the system. The binding free energy, as usually

defined, is expected to be stronger (more negative) in the absence of small ions than in their presence. In fact, this expectation is verified (see below). An interesting and counterintuitive influence of the small ions was nonetheless revealed by the simulation.

Usually, a binding free energy is referred to infinite distance; it measures the work required to move the binding molecules from a large separation distance to the docking, or bound, position. But suppose the binding free energy is redefined to mean the work required to move the λ repressor from a distance relatively close to the DNA into its docking position (which is still closer). This definition could actually be of more relevance in a biological context than the conventional definition. Jayaram et al. found that the presence of Na^+ and Cl^- ions acts to make the binding free energy, thus redefined, more negative; the redefined binding free energy is stronger in the presence of the small ions than in their absence. The effect is counterintuitive, because screening theory predicts that salt weakens the binding free energy of an oppositely charged ion pair, regardless of the starting distance between the ions.

The authors interpreted their result as reflecting the phenomenon of counterion release. When a charged ligand penetrates the layer of counterions condensed on an oppositely charged polyion, theory predicts that some of the condensed counterions will be released into bulk solution, providing an entropic contribution to the driving force for ligation.^{2,3} In the absence of small ions, there would be no condensed layer of counterions, and this source of favorable entropy (negative free energy) would be absent. Counterion release strengthens the direct attraction between oppositely charged ligand and polyion, and if it is assumed to be the dominating influence of small ions at

(1) Jayaram, B.; DiCapua, F. M.; Beveridge, D. L. *J. Am. Chem. Soc.* **1991**, *113*, 5211–5215.

(2) Manning, G. S.; Ray, J. *J. Biomol. Struct. Dyn.* **1998**, *16*, 461–476.

(3) Ray, J.; Manning, G. S. *Macromolecules* **1999**, *32*, 4588–4595.

near distances, then the negative free energy observed in the simulation can be understood. The interpretation of Jayaram et al. is all the more reasonable, since, as they point out, the maximum enhancement of the binding (from close distances) is observed to occur when the protein is at a distance corresponding to the width of the condensed layer of counterions, the latter having been clearly demarcated by an inflection point in the counterion distributions measured in earlier simulations.^{4,5} The existence of a layer of counterions condensed in the strict sense of “charge renormalization” has been strikingly confirmed by a combination of small-angle X-ray and small-angle neutron scattering.⁶ The current direction of our own research into polyelectrolyte behavior^{2,3,7,8} puts us in a good position to calculate the simulated small-ion effect by analytical theory, and we thought it would be interesting to see if we could validate the reasonable but essentially speculative interpretation of the simulation as a reflection of counterion release.

2. The JDB Salt Effect Function

2.1. Definition. In the Monte Carlo simulation of Jayaram et al.,¹ explicit Na⁺ and Cl⁻ ions are present in addition to the repressor protein and the DNA operator site. The simulated aqueous solvent is represented by a continuum dielectric coefficient provided with a distance dependence for greater realism at close distances. The DNA has negatively charged phosphate groups P, and the protein has both positively charged lysine and arginine residues and negatively charged glutamate and aspartate residues, generically symbolized as R. The input in the simulation is a set of direct Coulomb interactions u_{ij} (with an r^{-12} repulsive core) between pairs of charges $\{ij\}$. All interactions involving small ions are included, i.e., u_{P-Na} , u_{P-Cl} , u_{R-Na} , u_{R-Cl} , u_{Na-Na} , u_{Cl-Na} , and u_{Cl-Cl} . But the direct protein–DNA interactions u_{P-R} are omitted (as well as the irrelevant PP and RR interactions). Thus, the authors simulate the effect of small ions on the repressor–operator energetics in isolation from the direct protein–DNA interaction.

A computation is carried out for a fixed distance r between protein and DNA, mutually oriented as in the actual bound complex, and results for a family of computations, each corresponding to a different value of r , are reported. A natural reference state for the simulation is the complex itself, the structure of which is available from crystallographic data. Thus, the reference state is not the conventional one at large separations, and the value of the free energy reported for distance r then represents the contribution of small ions to the work required to bring the protein from distance r to its final “docking” position. In our theoretical free energy, which we wish to compare to the simulated free energy, we will also use the docked position as reference.

Let $w(r)$ be the usual potential of mean force for some pair of charged particles A and B that we wish to study. Its reference state is at infinity, $w(\infty) = 0$, so that $w(r)$ is the work required to bring A and B from infinite separation to separation distance r in the presence of small ions. Let $u(r)$ be the direct potential for this pair (in the absence of small ions). If the direct potential is subtracted out of the overall potential, then what is left,

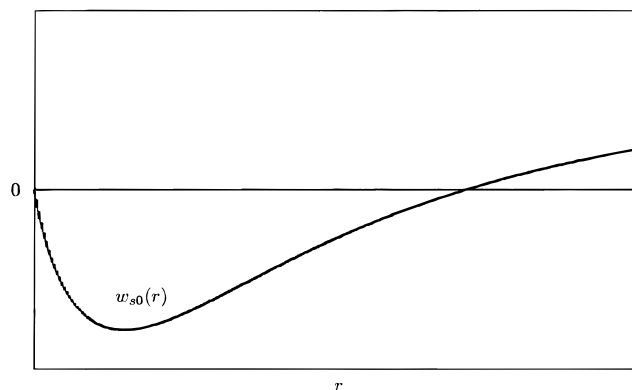


Figure 1. Schematic plot illustrating the results of the JDB simulation.

namely, $w(r) - u(r)$, is the effect of small ions on the work required to bring the pair from infinite separation to r . As noted, we change the reference state by letting a be some cutoff distance of closest approach. Then the small-ion effect on the overall work $w(a) - w(r)$ required to bring A and B from separation distance r to a is given by the formula

$$w_{s0}(r) = [w(a) - u(a)] - [w(r) - u(r)] \quad (1)$$

The subscript “s” in the function $w_{s0}(r)$ representing the small-ion effect reminds us of “salt”, a term intended to apply to all small ions in the system, inclusive of the DNA and protein counterions as well as of any added NaCl; the subscript 0 refers to the choice of reference state (which, if not zero, is at least the distance of closest approach of A and B). We will refer to the energy function $w_{s0}(r)$ as the JDB salt effect function, after the authors of the motivating simulation.¹

To develop insight into the JDB function as defined in eq 1, we look first at the case of infinite r . For well-behaved potentials, both $w(\infty)$ and $u(\infty)$ vanish, and $w_{s0}(\infty)$ reduces to $w(a) - u(a)$, that is, the effect of small ions on the binding free energy as conventionally defined (the work involved in moving the binding particles from infinity to their bound state). Both the JDB simulation and our calculated results provide positive values for $w_{s0}(r)$ when r is large, in accord with the expectation that the presence of small ions weakens the attractive free energy of binding from distant separation. Next, we note that the function $w(r) - u(r)$, which gives the effect of small ions on the conventional potential at r , may be obtained by flipping the JDB function about the horizontal axis (i.e., changing its sign) with a vertical shift to the value 0 at ∞ . Then $w(r) - u(r)$ can be seen to be positive for all r in the JDB simulation and in all cases studied in this paper, whatever the appearance of the JDB function. Thus, the presence of small ions always weakens the attractive potential at every distance relative to infinite separation. Finally, at the cutoff $r = a$, eq 1 reports $w_{s0}(a) = 0$ as the trivial consequence of the choice of reference state in the definition of the JDB energy as the distance corresponding to the bound state.

Attention is now directed to Figure 1, where we give a schematic drawing of the result of the JDB simulation. In a range of close distances r , the JDB function $w_{s0}(r)$ is negative. This means that the small ions in the system act to strengthen the attractive free energy of binding, redefined to mean the work required to bind the protein starting from distance r . Another way to interpret Figure 1 is to consider the negative slope of $w_{s0}(r)$, which extends from $r = 0$ to the value of r where the function has its minimum. If we differentiate both sides of eq 1 with respect to r , we will see that a negative value for the

(4) Jayaram, B.; Swaminathan, S.; Beveridge, D. L.; Sharp, K.; Honig, B. *Macromolecules* **1990**, *23*, 3156–3165.

(5) Young, M. A.; Jayaram, B.; Beveridge, D. L. *J. Am. Chem. Soc.* **1997**, *119*, 59–69.

(6) Essafi, W.; Lafuma, F.; Williams, C. E. *Eur. Phys. J. B* **1999**, *9*, 261–266.

(7) Manning, G. S. *Ber. Bunsen-Ges. Phys. Chem.* **1996**, *100*, 909–922.

(8) Manning, G. S. *Physica A* **1996**, *231*, 236–253.

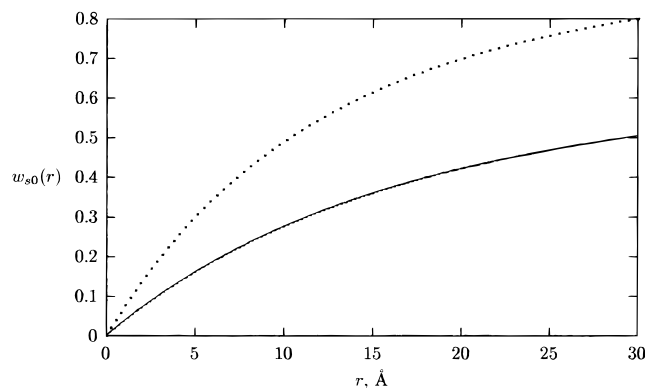


Figure 2. JDB function $w_{s0}(r)$ in units of RT for a pair of oppositely charged univalent point ions in Debye–Hückel theory. Solid curve, 0.1 M salt; dotted curve, 0.2 M salt.

slope of $w_{s0}(r)$ means that the force between protein and DNA in the presence of small ions is less than in their absence. For an attractive interaction, the force is a negative number, so “less than” in this context means a negative value of greater magnitude. The presence of small ions makes the attractive force larger in this range of distances. From either standpoint—energy or force—the physical significance of the negative region of the JDB function shown in Figure 1 runs counter to expectation from simple screening of an attracting pair of oppositely charged ions (see Figure 2 with accompanying analysis below).

2.2. The JDB Function in Debye–Hückel Theory. In this section we try to deepen our insight into the JDB salt effect function by deriving Debye–Hückel limiting laws for several pertinent examples. Let us start with the interaction between a pair of oppositely charged univalent ions A^+ and B^- immersed in an aqueous NaCl solution. We measure potentials in units of $k_B T$ (Boltzmann constant times Kelvin temperature). The potentials contain the factor q^2/D , where q is the unit charge and D the dielectric constant of bulk water, and it is convenient to use the Bjerrum length λ , given in esu-cgs units, by

$$\lambda \text{ (cm)} = q^2/Dk_B T \quad (2)$$

about equal to 7.1 Å in water at room temperature. The Debye–Hückel limiting law expressing the potential of mean force for ions A^+ and B^- separated by distance r is a screened Coulomb potential,

$$w(r) = -(\lambda/r) \exp(-\kappa r) \quad (3)$$

where κ is the inverse Debye length of the NaCl solution,

$$\kappa^2 \text{ (cm}^{-2}\text{)} = 8\pi\lambda(L_{Av}/1000)c_{NaCl} \quad (4)$$

where L_{Av} is Avogadro’s number and c_{NaCl} is the salt concentration in molarity units. The value of $1/\kappa$ is about equal to 30.5 Å in aqueous 0.01 M NaCl solution. The direct Coulomb potential for A^+ and B^- is

$$u(r) = -\lambda/r \quad (5)$$

The potentials may be evaluated both at r and at $r = a$ and the corresponding expressions substituted into eq 1. After this step, the simplifying limit $a \rightarrow 0$ may be implemented without encountering a singularity. The result is

$$w_{s0}(r) = \lambda \frac{e^{-\kappa r} + \kappa r - 1}{r} \quad (6)$$

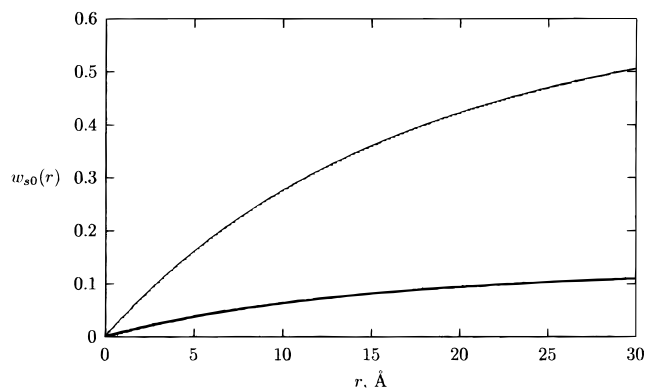


Figure 3. JDB function (heavy curve, Debye–Hückel theory) in units of RT for a bipolar ion of length 4 Å approaching a univalent point ion, the oppositely charged end of the bipolar ion coming head-first at distance r from the point ion. The light curve for an approaching pair of point ions is included for comparison and is taken from Figure 1. The salt concentration for both curves is 0.1 M.

We restate the meaning of $w_{s0}(r)$ in the context of the present example. The ions A^+ and B^- , conceptualized as structureless points, are brought from distance r to zero distance in an aqueous NaCl solution. A certain amount of negative work is done in this process (indeed, the work is negatively infinite). The JDB function $w_{s0}(r)$ gives the effect of the ion atmospheres on this work in the framework of Debye–Hückel limiting law theory. The contribution of the ion atmospheres is not infinite.

We show in Figure 2 plots of $w_{s0}(r)$ for two different salt concentrations according to eq 6. Note that $w_{s0}(r)$ is everywhere positive. The effect of the ion atmospheres is to make the overall negative work less negative; the presence of salt acts to diminish the direct attractive force between the A^+ and B^- charges. Indeed, Figure 2 is an effective way to illustrate Debye–Hückel screening. The second thing to notice is that the screening is greater for the higher salt concentration.

As a second example, we continue to let the charged entity B be a univalent negative ion B^- , which now we might want to think of as an isolated phosphate group on DNA. For species A we choose an amino acid, represented as a bipolar ion with a unit positive charge at one end and a unit negative charge on the other end, separated by a rigid spacing l . The bipolar ion A is allowed to approach B^- radially with its positive end coming first; in other words, the distance between the positive end and B^- is r , and the distance between the negative end and B^- is $r + l$. The potentials w and u of eqs 3 and 5 may be applied to each end of the bipolar ion (with a sign change for the potential between B^- and the negative end of the bipolar ion), and the result for the JDB salt effect function from eq 1 is

$$w_{s0}(r) = \lambda \frac{e^{-\kappa r} + \kappa r - 1}{r} + \lambda \frac{e^{-\kappa l}(r + l - l e^{-\kappa r}) - r}{l(r + l)} \quad (7)$$

In this equation we have again taken the limit of zero cutoff distance, so $w_{s0}(r)$ gives the effect of salt on the work required to bring the point positive charge at one end of A from distance r to the location of the point charge B^- , the negative end of A trailing along radially. Note that there is no need to consider the intramolecular interaction between the two ends of the bipolar ion, because it would cancel in the difference between the initial and final states.

In Figure 3 we show one of the curves from Figure 2 for the approach of a counterion A^+ to B^- together with a plot of eq 7 for the approach of an amino acid A to B^- in aqueous NaCl of the same concentration. The salt effect for the latter situation

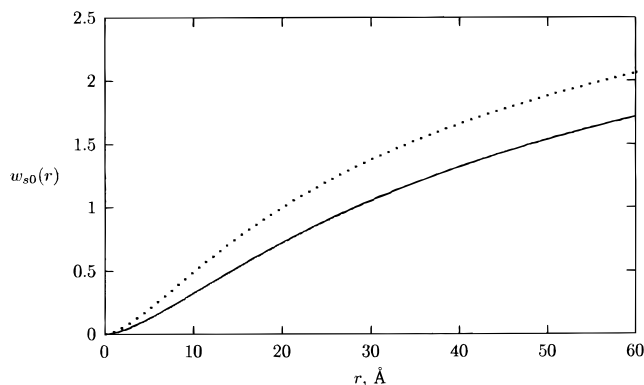


Figure 4. JDB function in units of $2\xi RT$ for a univalent counterion approaching a line charge in Debye–Hückel theory. In these units, the graph is the same for any line charge density ξ . Solid curve, 0.1 M salt; dotted curve, 0.2 M salt.

is qualitatively the same as that for the former. Since the positive end of the bipolar ion is closer to B^- than the negative end, the behavior of A is qualitatively that of a cation. However, the negative end of A does interact repulsively with B^- , so the overall electrostatic interaction of the net zero charge of A with B^- is substantially less than that for an unmitigated cation.

For our next example, let species A be a point counterion A^+ and B an infinite negative line charge of unsigned reduced charge density ξ :

$$\xi = \lambda/b \quad (8)$$

wherein a line segment of length b contains a unit amount of charge. Recalling that b is about 1.7 \AA for the solution structure of DNA, we see that ξ for DNA is about 4.2, which is quite large. The use of Debye–Hückel theory would be accurate only for sufficiently small values of ξ , but in this section we are not so much interested in accuracy as we are in gaining qualitative understanding.

The potential of mean force for A and B in units of $k_B T$ as given by Debye–Hückel limiting law theory is

$$w(r) = -2\xi K_0(\kappa r) \quad (9)$$

where K_0 is the Bessel K function (modified Bessel function of the second kind) of order zero, and the direct potential is

$$u(r) = 2\xi \ln r \quad (10)$$

After substitution of eq 10 into eq 1, we pass to the limit of vanishing cutoff a without encountering a singularity, and find

$$w_{s0}(r) = 2\xi[-\ln 2 + \gamma + K_0(\kappa r) + \ln(\kappa r)] \quad (11)$$

where γ is the Euler constant, $\gamma = 0.5772\dots$ Figure 4 illustrates the present case. Once again, we have ordinary screening behavior.

In the final example of this section, the negative line charge B interacts with bipolar ion (amino acid) A possessing positive and negative ends separated by rigid spacing l . The bipolar ion approaches the line charge in radial orientation with its positive end head-on. The distance between the positive end of A and the line charge is equal to r , and the distance of the negative end from the line charge is therefore equal to $r + l$. The Debye–Hückel JDB salt effect with cutoff a taken to zero is derived as

$$w_{s0}(r) = 2\xi\{-\ln 2 + \gamma + K_0(\kappa r) + K_0(\kappa l) - K_0[\kappa(r+l)] + \ln(\kappa r) - \ln[(r+l)/l]\} \quad (12)$$

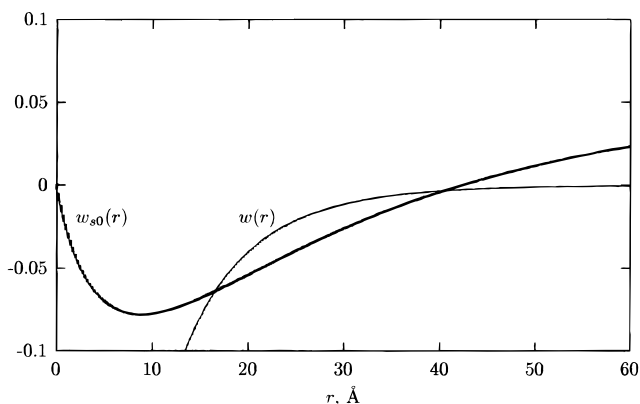


Figure 5. JDB function $w_{s0}(r)$ (heavy curve, Debye–Hückel theory) in units of $2\xi RT$ for a bipolar ion of length 4 \AA approaching a line charge, the oppositely charged end of the bipolar ion coming head-first at distance r from the line. The light curve is the potential of mean force $w(r)$ for this case with the same units (the descent is monotonic even to the left of the portion of the curve shown). The salt concentration for both curves is 0.1 M.

Figure 5 presents a graph of $w_{s0}(r)/2\xi$ and reveals a feature that we did not expect: the curve descends with increasing r into negative values before hitting a minimum and rising into a positive region of ordinary screening. Note from eq 12 that the charge density ξ merely plays the role of a scaling factor, as it must in linear Debye–Hückel theory. The minimum is therefore present even at low charge densities where Debye–Hückel theory is accurate. As part of Figure 5 we have shown a plot of the ordinary potential of mean force for this case, $w(r)/2\xi = -K_0(\kappa r) + K_0[\kappa(r+l)]$. This plot exhibits an apparently ordinary screened Coulomb attraction. The bipolar ion approaching the anionic line charge with cationic end head foremost looks like a cation when analyzed with the overall potential of mean force but not when viewed through the JDB salt energy function.

Negative values of the JDB function mean that the direct attractive force between two ionic particles is enhanced by salt at short distances. One might not have guessed that w_{s0} could have negative values in limiting law Debye–Hückel theory. How can we interpret it? The positive end of the bipolar ion is closer to the negative line charge than the negative end. The positive end is therefore less screened from the negative line charge than is the negative end. The salt exerts a stronger screening effect on the repulsive interaction between the more distant negative end and the negative line charge than it does on the closer attraction of the positive end. The free energy of screening is therefore net negative (diminishing the repulsive component), at least at shorter distances, where the overall interaction is large. A rough numerical analysis (not shown) does, in fact, indicate a strong correlation of the location of the minimum with the Debye screening length, $r_{\min} \approx 1.11\kappa^{-1}$.

The interpretation of the previous paragraph cannot be the whole story, since the same logic would apply to the salt effect on the radial approach of a bipolar ion to a point charge. But Figure 3 shows only positive values of the corresponding function w_{s0} and no minimum. We are grateful to a reviewer for pointing out that nothing as complicated as a line charge is needed to illustrate negative values of w_{s0} . Although the radial approach of a bipolar ion to a point charge generates only positive values at all distances, the approach of a bipolar ion to an offset point charge produces a JDB function that looks like the one in Figure 5 (for example, a bipolar ion with positive end head-on approaches the origin along the x -axis, while a

negative point charge is fixed, not at the origin, but at some nonzero point on the y -axis). Subtle distance dependencies are involved. Note that although the line charge is not present in this example, the approaching ion is bipolar, with its distant negative end repelling the targeted negative charge.

A line charge is important to our considerations, because it will serve as our model for DNA. Debye–Hückel theory provides an accurate description of electrostatic interactions involving line charges of sufficiently low charge density. We have learned, therefore, that small ion enhancement of the direct attraction at short distances between a line charge of low charge density and a bipolar ion approaching with counterionic end head-first occurs, but (1) is not associated with counterion release from a condensed layer, since a condensed layer of counterions is absent from limiting law Debye–Hückel theory, and (2) is associated with the repulsion between the line charge and the trailing co-ionic end of the bipolar ion, since the enhancement effect does not occur when a pure counterion approaches the line charge (Figure 4).

2.3. Counterion Release. The plots of w_{s0} in Figure 5 are similar in appearance to the simulated data of Jayaram et al.¹ for the λ repressor–operator interaction (compare with Figure 1). The DNA operator site, however, has a high charge density, about 4 times the threshold value for emergence of a condensed layer of counterions. Unmodified Debye–Hückel theory can be characterized not merely as inaccurate at such high charge densities but qualitatively inapplicable, since it does not provide the condensed counterions that dominate so many aspects of polyelectrolyte behavior. In particular, counterions are released from the condensed layer surrounding DNA when basic (positively charged) protein residues penetrate the layer. To determine the effect of the presence of these ions on the free energy of attraction, we need a potential of mean force $w(r)$ that is applicable at high charge densities. In this section we study the attraction of a point counterion to a line charge (more precisely, a linear array of discrete charged points) by means of a potential appropriate to charge densities above the threshold condensation value.

An ion–polyion potential of mean force, the work required to bring a line charge and a point Z -valent ion of opposite sign from infinity to r , has been derived previously in the framework of counterion condensation theory.³ Separate expressions for $w(r)$ apply to three disjoint ranges of distances r . The near range extends out from the line charge to distance $r = (1/e)\kappa^{-1}$, where e is the base of natural logarithms. An intermediate range runs from $r = (1/e)\kappa^{-1}$ to $r = \kappa^{-1}$. Both the near and intermediate ranges are therefore inside a Debye length. Counterions in the near region correspond to the condensed layer.³ Space is completed by a far region, outside the Debye length, reaching to infinity from $r = \kappa^{-1}$. The theoretical potential is continuous across the near–intermediate and intermediate–far interfaces. The joining conditions are treated approximately, however, and the potential is not smooth across the interfaces. The following formulas are for the pair potential between a line charge and a Z -valent oppositely charged ion brought from infinity to r in background 1–1 salt like NaCl. If the line charge is negative, the counterions are Na^+ ions. The threshold for condensation is therefore $\xi = 1$, and the formulas are applicable for $\xi > 1$. The Z -valent ion can be (but is not necessarily) a singled-out Na^+ .

Near region:

$$Z^{-1}w(r) = -2\xi K_0(\kappa r) - 2(\xi - 1) \ln(\kappa b) + 1 \quad (13)$$

Intermediate region:

$$Z^{-1}w(r) = -2\xi K_0(\kappa r) + 2(\xi - 1) \ln(\kappa r) \ln(\kappa b) - \ln(\kappa r) \quad (14)$$

Far region:

$$Z^{-1}w(r) = -2\xi K_0(\kappa r) \quad (15)$$

In the first two of these formulas, b is the spacing of the linear array of charges modeling the polyion. Note that in the far region, $Z^{-1}w(r)$ is given by a Debye–Hückel formula even though $\xi > 1$. This surprising result (one might have thought that a counterion at a far distance r would see only the net charge on the polyion, intrinsic charge minus charge of condensed layer, $\xi_{\text{net}} = 1$) stems from cancellation of two distinct nonlinear effects.³

Along with these formulas for $w(r)$, the number of condensed counterions can also be calculated as a function of position r of the Z -valent ion. If P is the number of charges on the polyion and θ the number of condensed counterions per polyion charge, then $P\theta$ is the number of condensed counterions. When the Z -valent counterion is at infinity, $P\theta = P(1 - \xi^{-1})$, a value that is maintained as the Z -valent counterion approaches to a far distance r . When the Z -valent counterion penetrates inside the Debye–Hückel cloud, i.e., into the intermediate region, $P\theta$ decreases:

$$P\theta(r) = P(1 - \xi^{-1}) + Z \ln(\kappa r) \quad (16)$$

This equation tells us that when the Z -valent ion has encroached upon the far–intermediate interface $r = \kappa^{-1}$, the number of condensed counterions is $P(1 - \xi^{-1})$. As the Z -valent ion penetrates up to the near–intermediate interface $r = (1/e)\kappa^{-1}$, the number of condensed counterions progressively decreases to the value $P(1 - \xi^{-1}) - Z$, that is, ultimately Z univalent counterions are released from the condensed layer. The number of released counterions does not increase further as the Z -valent ion penetrates into the near region up to the position of the polyion. The main point here is that the potential of mean force $w(r)$ contains the effect of released counterions.

An unusual feature of $w(r)$ merits graphical illustration. Figure 6 shows plots of $Z^{-1}w(r)$, which is independent of Z , for two salt concentrations. The three regions are clearly visible (because the approximate joining conditions could not produce a smooth curve). A free energy barrier impedes progress of the Z -valent ion toward the polyion. If the Z -valent ion is a singled-out univalent counterion, the barrier generates two distinct peaks in the counterion radial distribution function, an inner one corresponding to the condensed layer, and an outer one corresponding to the Debye–Hückel cloud.³ Both the attraction in the far region and the repulsion in the intermediate region are stronger for the lower concentration. There is little dependence on salt in the near region (condensed layer).

Corresponding results for the JDB salt effect function are readily obtained. The direct potential $u(r)$ (divided by Z) is given by eq 10. For the present case, eq 1 for the JDB function becomes

$$w_{s0}(r) = [w_{\text{near}}(a) - u(a)] - [w(r) - u(r)] \quad (17)$$

where $w_{\text{near}}(a)$ is the potential evaluated at the cutoff distance a , reasonably taken as less than $(1/e)\kappa^{-1}$, and hence in the near

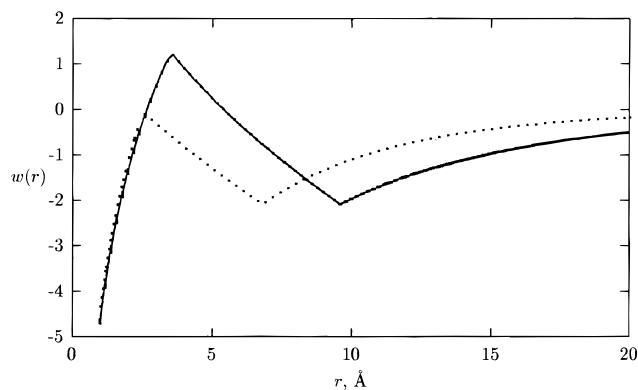


Figure 6. Potential of mean force $w(r)$ in units of ZRT for a Z -valent counterion approaching a line charge in counterion condensation theory. In these units, the graph is the same for any value of Z . Solid curve, 0.1 M salt; dotted curve, 0.2 M salt. The charge density of the line, $\xi = 4.2$, is that of DNA and corresponds to charge spacing $b = 1.7 \text{ \AA}$.

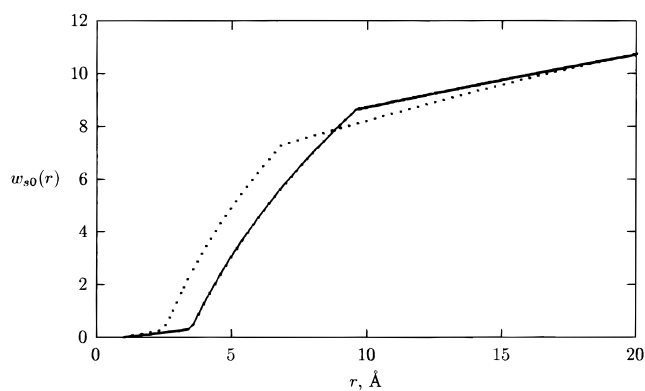


Figure 7. JDB function in units of ZRT for a Z -valent counterion approaching a line charge ($\xi = 4.2$, $b = 1.7 \text{ \AA}$) in counterion condensation theory. Solid curve, 0.1 M salt; dotted curve, 0.2 M salt.

region. In any event, when we go to the limit $a \rightarrow 0$, the following expressions emerge:

Near region:

$$Z^{-1}w_{s0}(r) = 2\xi[K_0(\kappa r) + \ln(\kappa r) - \ln 2 + \gamma] \quad (18)$$

Intermediate region:

$$Z^{-1}w_{s0}(r) = 2\xi[K_0(\kappa r) + \ln(\kappa r) - \ln 2 + \gamma] - 2(\xi - 1) \ln(\kappa b)[\ln(\kappa r) + 1] + \ln(\kappa r) + 1 \quad (19)$$

Far region:

$$Z^{-1}w_{s0}(r) = 2\xi[K_0(\kappa r) + \ln(\kappa r) - \ln 2 + \gamma] - 2(\xi - 1) \ln(\kappa b) + 1 \quad (20)$$

Figure 7 gives a plot of $Z^{-1}w_{s0}(r)$ in accordance with eqs 18–20. The graph is the same for any value of Z . Perhaps its single most striking aspect is that it looks very much like the one in Figure 4, showing ordinary Debye–Hückel screening for the same system (interaction between a line charge and a point charge of opposite sign). The effect of counterion release is indubitably incorporated into our formulas and certainly gives a negative contribution to $w_{s0}(r)$. It must be offset by other effects that weaken the inherent attraction of the ion–polyion pair. It is not easy to pick these equations apart into their constituent physical contributions. One way to rationalize our result begins by noting that counterion release occurs progressively as the Z -valent point ion approaches the oppositely

charged line across the intermediate region. The intermediate region is characterized by partial screening [this statement is a precise one,³ but it is also intuitively clear from the fact that the values of r in this region lie between $(1/e)\kappa^{-1}$ and κ^{-1}]. The unfavorable effect of partial screening on the attraction may dominate the favorable free energy of counterion release. The process of counterion release is finished when the Z -valent ion arrives at the near–intermediate interface. No further release of counterions occurs when the ion penetrates and crosses the near region. Correspondingly, there is essentially no screening within the near region (again, a precise statement³), and $w_{s0}(r)$ in Figure 7 can be seen to be close to zero in this region.

There is one difference between Figures 7 and 4, and it concerns the salt dependence. For ordinary Debye–Hückel screening as illustrated in Figure 4, raising the salt concentration increases the amount of screening at all distances r between counterion and line charge. In contrast, Figure 7 for the full counterion condensation theory of the counterion–polyion interaction shows a crossover near the boundary between intermediate and far regions. There exists a region in Figure 7 where higher salt concentration weakens the direct attractive interaction between counterion and polyion less than lower salt. The curves in Figure 7 cross back to the “normal” order at a value of r well into the far region.

The counterion condensation theory is actually more complicated than is sometimes supposed. In particular, the presence of a Z -valent ion at r perturbs the internal partition function of the counterions condensed on the line charge.³ This effect is present in the theory, it exists in addition to the effects of counterion release and screening, and it is important. We find it hard to tell how it affects the qualitative features of Figure 7. We may firmly conclude, however, that the negative values of the JDB free energy found by Jayaram et al.¹ in their simulation of the λ repressor–operator system cannot be explained solely as a manifestation of the favorable free energy generated by release of condensed Na^+ ions when a cationic protein residue penetrates the condensed layer.

2.4. Modeling a Protein–DNA Interaction. In this section we look at two models of a protein–DNA interaction in the framework of counterion condensation theory. The DNA is represented as a negatively charged line (i.e., a linear array of point negative charges with spacing b). In the first model, the “protein” is the bipolar ion whose interaction with a line charge was analyzed above with limiting law Debye–Hückel theory (Figure 5). The second model for the protein is a large collection of positive and negative charges, given the coordinates of the basic and acidic charged groups of λ repressor protein.

The interaction among a collection of charges is not generally pairwise additive in counterion condensation theory. For example, the free energy of assembly of three line charges in parallel array does not equal the sum of the free energies of assembling the three pairs of line charges, each pair of charges in isolation from the third charge.⁹ In the present case, the question arises of whether we can equate the interaction free energy of the line charge and the several charged sites on the protein to the sum of the free energies of interaction of the line charge with each of the charged protein sites considered in isolation from the others. It turns out that we cannot. The overall intermolecular potential of a negative line charge and a counterion–co-ion pair is not equal to $w_+(r_+) + w_-(r_-)$, where the first term is the potential for the isolated counterion at r_+ and the second is the potential for the isolated co-ion at r_- . What is true, however, is fortunately even simpler. The potential

(9) Ray, J.; Manning, G. S. *Macromolecules* **2000**, *33*, 2901–2908.

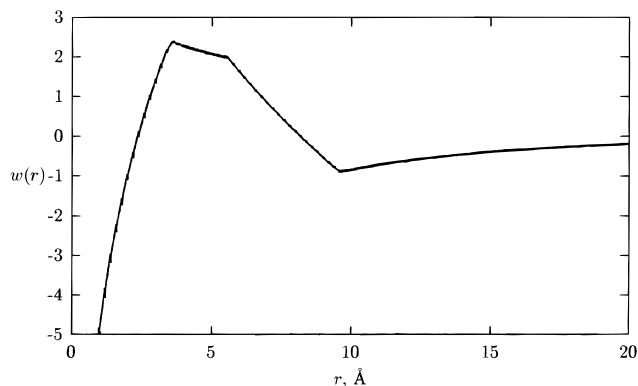


Figure 8. Potential of mean force $w(r)$ (counterion condensation theory) in units of RT for a bipolar ion of length 4 \AA approaching a line charge ($\xi = 4.2$, $b = 1.7 \text{ \AA}$), the oppositely charged end of the bipolar ion coming head-first at distance r from the line. The ionic strength is 0.1 M .

for this case equals $w_+(r_+) - w_+(r_-)$. In other words, there is additivity if we set the potential for the co-ion equal to the potential for the counterion with changed sign, just as we would in the context of Coulomb's law or Debye–Hückel theory. The argument is given in the Appendix.

2.4.1. Bipolar Ion. In this paragraph we continue our consideration of the counterion–co-ion pair, or bipolar ion. A point positive charge attached to a point negative charge with rigid spacing l approaches a negative line charge in radial orientation with the positive end head-on. The potentials are expressed as functions of the distance r between the positive end and the line charge. The negative end is always at distance $r + l$ from the line charge. Several regions of a “direct product” space arise. For example, the positive end of the bipolar ion can be in the near region, while the negative end is in the intermediate region. A complete list of the six possibilities is near–near, near–intermediate, near–far, intermediate–intermediate, intermediate–far, and far–far. Of these six, only two are always present regardless of the values of the bipolar ion spacing l and the Debye screening length κ^{-1} : the intermediate–far and far–far regions. The near–near region is present only if $l < (1/e)\kappa^{-1}$. The near–intermediate region is present only if $l < \kappa^{-1}$. The near–far region is present only if $l > \kappa^{-1}(1 - e^{-1})$ (the width of the intermediate region). Finally, the intermediate–intermediate region is present only if $l < \kappa^{-1}(1 - e^{-1})$. Thus, a very short bipolar ion passes through five of the six regions as it moves away from the line charge to infinity (all but the near–far region), while a very long bipolar ion encounters only three (the near–far, intermediate–far, and far–far regions).

The pseudoadditivity discussed above makes it easy to write down the potential of mean force (work required to bring the bipolar ion from infinity to r) in each region. With the abbreviations $n = \text{near}$, $i = \text{intermediate}$, and $f = \text{far}$, let for example $w_{ni}(r)$ be the potential when the positive end is in the near region at r and the negative end is in the intermediate region at $r + l$. Then, $w_{ni}(r) = w_n(r) - w_i(r + l)$, where $w_n(r)$ is given by the right-hand side of eq 13, and $w_i(r + l)$ is the expression on the right-hand side of eq 14 but evaluated at $r + l$ instead of r .

Figure 8 illustrates the potential when $l = 4 \text{ \AA}$ and $\kappa^{-1} = 9.6 \text{ \AA}$ (0.1 M NaCl). The boundary between near and intermediate regions is at $(1/e)\kappa^{-1} = 3.5 \text{ \AA}$, so as r moves from a cutoff, say, of 1 \AA ,³ the potential $w(r)$ passes successively through the branches $w_{ni}(r)$ ($1 \leq r \leq 3.5$), $w_{ii}(r)$ ($3.5 \leq r \leq 5.6$), $w_{if}(r)$ ($5.6 \leq r \leq 9.6$), and $w_{ff}(r)$ ($9.6 < r < \infty$). Figure 8 may be compared

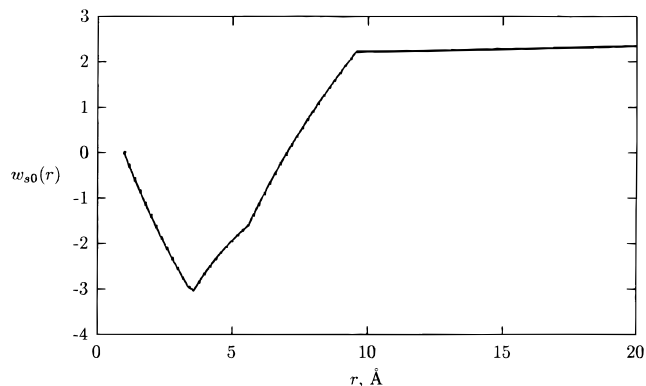


Figure 9. JDB function (counterion condensation theory) in units of RT for a bipolar ion of length 4 \AA approaching a line charge ($\xi = 4.2$, $b = 1.7 \text{ \AA}$), the oppositely charged end of the bipolar ion coming head-first at distance r from the line. The ionic strength is 0.1 M .

with Figure 6 for the potential of mean force of a counterion and the line charge. The qualitative features of the potentials are similar for the particular numerical values of the parameters chosen, although differences in detail are evident.

In the calculation of the JDB salt free energy w_{s0} , we have to realize that the reference state is at $r = 0$ for the positive end of the bipolar ion but at $r = l$ for the negative end. Thus, in the near–intermediate region we get

$$w_{s0}^{ni}(r) = w_{s0}^n(r) + w_{s0}^i(l) - w_{s0}^i(r + l) \quad (21)$$

where w_{s0}^α ($\alpha = n, i, f$) is the salt effect function for a point counterion (isolated positive end of the bipolar ion) in the near, intermediate, or far region, as given by eqs 18, 19, and 20, respectively, with $Z = 1$. The negative end of the bipolar ion is accounted for in the signs. The middle term of the right-hand side is always the same. For example, to obtain w_{s0}^{if} , replace n by i in the first term, leave the middle term unchanged, and replace i in the last term by f .

We illustrate the salt function in Figure 9. The graph is dominated by the minimum at negative values of the function. The decreasing portion is in the near–intermediate region. Now Figure 7 shows that the contribution to the salt function from the positive end in the near region is almost zero. The positive end is represented by the first term of the right-hand side in eq 21. The negative values in Figure 9 are generated by the middle and last terms. Both of these terms appear only because of the presence of the negatively charged end of the bipolar ion. Therefore, the negative values and the minimum in Figure 9 are caused by the presence of the negative end (same sign charge as the polyion) and are not correlated with the release of counterions from the condensed layer surrounding the polyion.

2.4.2. λ Repressor Protein. A protein typically contains many ionized groups, not just two. In the framework of our model, the problem is to calculate the potential of mean force between a line charge (the DNA) and a collection of unit positive and negative point charges all with fixed positions relative to each other (the protein). The problem is simplified by the pseudoadditivity discussed above and in the Appendix, but it is still complicated, because several protein charges may be in the near region, several in the intermediate region, and several in the far region; and the number of charges in each region, and the mix of charge types, changes as the distance between protein and DNA changes. In the “docked” position, i.e., in the protein–DNA complex, we ascertain from crystallographic data the distance d_i between each ionized protein residue i and its nearest

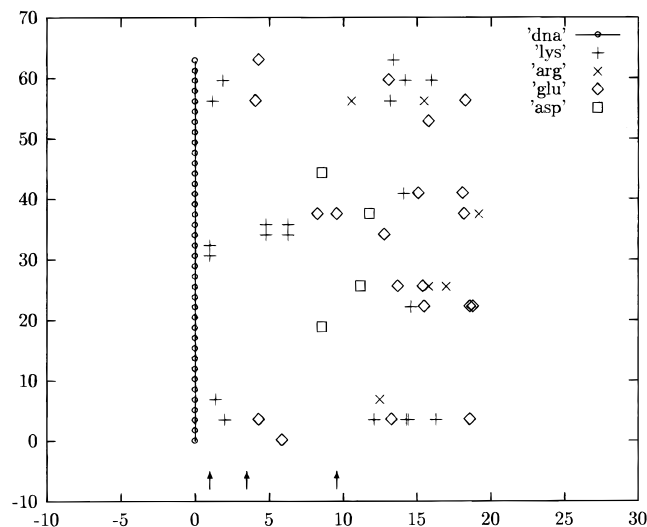


Figure 10. Two-dimensional model of the ionic interactions in the λ repressor–operator complex. The numbers on the axes are distances in angstroms. The DNA phosphates are spaced at 1.7 Å. The cutoff distance a (left arrow) is at 1 Å. The near region lies between the left and center arrows, the intermediate region is between the center and right arrows, and the far region extends beyond the right arrow (a Debye length from the DNA). The near–intermediate and intermediate–far boundaries depend on ionic strength; the positions shown correspond to 0.1 M.

DNA phosphate. In our model, the protein charge $i = 0$ closest to a DNA phosphate is placed at a cutoff distance a from the line charge representing the DNA. The distance of any other protein charge i is then set to $a + d_i - d_0$. Then when we say that the protein is at a distance r from the DNA, we mean that the distance r has been added to the docking distance of each protein charge. We have written an algorithm that generalizes the case of the protein as bipolar ion to the protein as a collection of an arbitrary number of positive and negative charges as described. It follows from the analysis given in the Appendix that the use of pseudoadditivity in the algorithm is justified if each negative charge either (1) can be paired with a positive charge closer to the DNA or (2) is so remote from the DNA that it finds itself in the far region even in the closest possible “docked” position of the protein.

In Figure 10, we show all the ionized protein residues (positively charged lysines and arginines, negative glutamic and aspartic acids) in the repressor–DNA complex as obtained from the Nucleic Acid Database (<http://ndbserver.rutgers.edu>, code PDR010). At the ionic strengths used in our calculations, 0.1 M NaCl and 0.2 M, the Debye screening lengths are 9.6 and 6.8 Å, respectively. The inside boundary of the far region at a specified ionic strength is given by the corresponding value of the screening length. It can be verified from Figure 10 that the conditions for applicability of our additivity-based algorithm are met. It should also be noted that the interface of the λ repressor–operator complex contains only positively charged protein residues. However, negatively charged groups are present in the intermediate region and even outnumber the positive charges there.

Figure 11 shows the ionic potential of mean force as a function of distance r between λ repressor and its DNA operator site. Comparison with Figures 6 and 8 reveals the similarity of the protein potential to that of a counterion or bipolar ion. The barrier to binding is prominent and creates a metastable position located well away from the absolute minimum at the binding site.

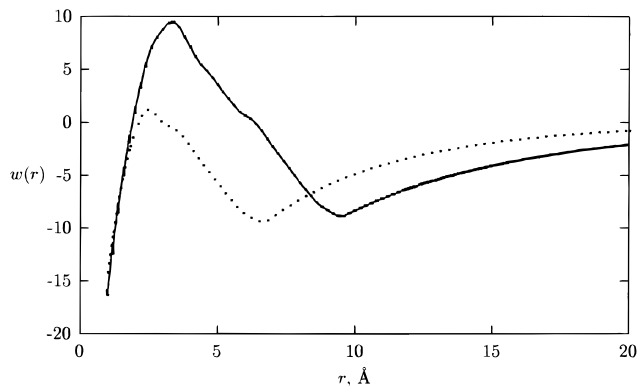


Figure 11. Potential of mean force $w(r)$ in kcal mol⁻¹ at 298 K for λ repressor and DNA in counterion condensation theory. Solid curve, 0.1 M salt; dotted curve, 0.2 M salt.

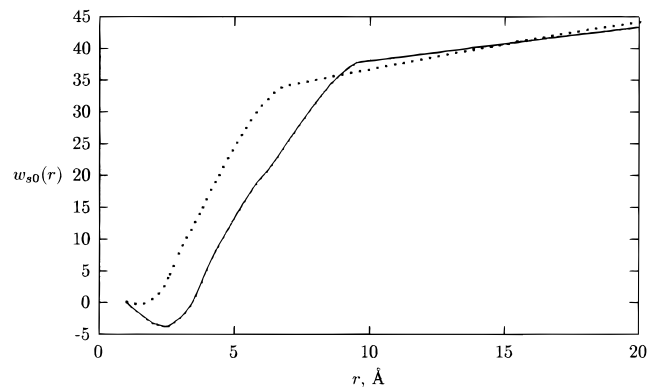


Figure 12. JDB function in kcal mol⁻¹ at 298 K for the λ repressor–DNA interaction in counterion condensation theory. Solid curve, 0.1 M salt; dotted curve, 0.2 M salt.

Figure 12 illustrates the calculated JDB salt effect function for the repressor–DNA interaction. Our model reproduces the minimum found by Jayaram et al.,¹ which we attribute to the influence of the co-ionic (negatively charged) protein residues in the range of intermediate distances from the DNA binding site. We agree with Jayaram et al. on the enhancement of the minimum at lower ionic strengths, and, like these authors, we also can see a crossover to an inverted salt dependence at larger distances. This long-distance feature is delicate, however; we do not see a crossover for all concentration pairs (not shown). Recall that the long-distance crossover is observed also in Figure 7 for the salt effect on the counterion potential.

Discussion

For the process of bringing two ionized molecules from an initial distance r to their final complexed position, we have defined a salt effect function $w_{s0}(r)$ to represent the contribution to the free energy change from interactions of the two reacting molecules with all other small ions also present in the solution. The function is defined to represent the same free energy as that computed by Jayaram et al.¹ in their Monte Carlo simulation of λ repressor and DNA operator. We have examined cases ranging from a simple ion-pairing reaction to the λ repressor–operator complexation.

If the reacting ions are of opposite sign, the prior expectation is for $w_{s0}(r)$ to be everywhere positive. The meaning of a positive value of $w_{s0}(r)$ for a given distance r is that the other small ions in the system act to weaken the direct attraction of the reacting ions. We expect this behavior from simple Debye–Hückel theory, which describes the effective weakening of an

ionic charge in solution by a surrounding screening atmosphere of net opposite charge. We indeed find the expected behavior for some of the systems we have looked at, such as an ion pair (Figure 2), the complexation of an ion with the oppositely charged end of an amino acid (Figure 3), and the complexation of an ion with an oppositely charged polyion (Figures 4 and 7). In connection with Figure 7, which illustrates the application of counterion condensation theory to the reaction of a Z-valent ion with an oppositely charged polyion, we noted that Z univalent counterions are released from the polyion when its condensed layer is penetrated by the Z-valent ion. The release of counterions contributes a favorable free energy to the binding of the Z-valent ion. Nonetheless, the overall effect of small ions in the solution, including the condensed counterions, is to weaken the attraction between the Z-valent ion and the polyion at all distances.

A dramatically unexpected effect is obtained, however, when a polyion binds the oppositely charged end of a bipolar amino acid, as analyzed either by Debye–Hückel or counterion condensation theory (Figures 5 and 9, respectively). For this case, the function $w_{s0}(r)$ descends from its reference value zero at the binding position into a range of negative values before reaching a minimum and then increasing into the familiar regime of positive values. A negative value of $w_{s0}(r)$ for some given distance r means that the direct attractive force at that distance between the polyion and the bipolar ion (which is oriented with its oppositely charged end closest to the polyion) is made stronger by the presence of the other small ions in the solution. We have identified the reason for this counterintuitive salt effect as reflecting the interaction of the polyion with the co-ionic end of the bipolar ion (the COO^- end of an amino acid binding to DNA, for example). The end of the bipolar ion bearing a charge of the same sign as the polyion is directly repelled by the polyion. The other small ions present in the system act to weaken the repulsion, thereby effectively strengthening the overall attraction between the polyion and the bipolar ion.

The action of small ions in augmenting a direct Coulomb attractive force, an effect exactly the opposite of expectation from Debye–Hückel screening considerations, persists in the case of the binding of the λ repressor protein to its operator site on DNA (Figure 12). Although in the protein–DNA bound complex the protein charges closest to the DNA are all positive (Figure 10), there are several negative protein charges at intermediate distances from the DNA phosphates. The co-ionic protein charges (glutamic and aspartic acid residues) are directly repelled by the phosphates. The direct repulsion is mitigated by the presence of Na^+ and Cl^- ions, which therefore favors the movement of the protein toward the DNA from relatively close separations. This fine-tuning of the protein–DNA interaction by negatively charged protein groups not in the binding site but not far from it points to a possible utility of these residues beyond maintenance of aqueous solubility.

We have also provided some results for the ordinary potential of mean force $w(r)$. This function gives the overall work required to bring two charged molecules from infinity to distance r , including the effect of interaction with all other ions in the system. Figure 5 contains an illustration of $w(r)$ as given by Debye–Hückel theory for the approach of a bipolar ion toward a polyion, the oppositely charged end coming first. The curve has the appearance of an ordinary screened Coulomb attraction. The application of counterion condensation theory gives a different result, as seen in Figure 6 for the interaction of a Z-valent ion and an oppositely charged polyion. A free energy barrier to binding is a prominent feature of $w(r)$. If the Z-valent

ion is a singled-out univalent counterion, the barrier causes separation of the counterions into two spatially separated populations, the condensed counterions on the near side of the barrier and the Debye–Hückel atmospheric counterions on the far side.³ For the approach of a bipolar ion to a polyion, the oppositely charged end coming first, counterion condensation theory as exhibited in Figure 8 again provides a barrier to binding of the oppositely charged end.

The barrier to binding persists for the λ repressor–DNA complex (Figure 11). Because the protein is attracted to its DNA destination at far distances, the barrier creates a deep (nearly 10 kcal) metastable position at its far side, well removed (7–10 Å) from the absolute minimum at the binding site. Possible transient storage of the protein at this remote local minimum should be kept in mind in any detailed consideration of the binding of λ repressor to its operator site, or of its release from the operator. Zacharias et al. have made a similar observation.¹⁰ The potential that we have calculated contains, of course, only the ionic protein–DNA interactions. On the other hand, the additional short-range interactions contributing to the overall potential of mean force may be too weak at distances removed from the binding site to distort significantly either the ionic barrier to binding or the remote minimum.

Although the minimum in the JDB function observed in Figure 12, and the crossover at far distances, are both in agreement with the simulation of Jayaram et al.,¹ we disagree on the magnitude of the salt effect at far separations. At far separations, the JDB function returns the effect of small ions on the free energy of binding starting from the separate species. Noting the high positive free energy values at large r in Figure 12, we can say that our calculated effect of salt (all small ions, including the counterions of the DNA and protein) is strongly unfavorable toward binding from the isolated species by about 40–45 kcal, whereas the simulated data of Jayaram et al. produce only a few kilocalories of unfavorable free energy (see their Figure 3). On the other hand, Misra et al.¹¹ have observed from numerical Poisson–Boltzmann calculations an unfavorable free energy of about 18 kcal due to the presence of small ions for the complexation of λ repressor and DNA operator; and from a completely different protocol, Jayaram et al. give an estimate of 132 kcal for the effect of small ions on complexation of this protein (B. Jayaram, private communication). Thus, we currently have estimates of the effect of small ions on λ repressor–operator binding (from the protein and DNA species either isolated or at large distances), all of which represent unfavorable free energy but range from a few kilocalories to over 100 kcal. Our estimate of 40–45 kcal is somewhere in the middle.

Acknowledgment. We are grateful to B. Jayaram for extended correspondence and to the U.S. Public Health Service for partial support of our research through Grant GM36284.

Appendix

If a polyelectrolyte solution is treated within Debye–Hückel theory, the counterion and co-ion potentials are everywhere essentially the same. Both equal the product of their respective charges with the electrostatic potential set up by the polyion. They differ, therefore, only in their sign. In counterion condensation theory, however, the counterion and co-ion potentials differ in a more fundamental way, at least in the near and intermediate regions.³ A co-ion positioned inside the near

(10) Zacharias, M.; Luty, B. A.; Davis, M. E.; McCammon, J. A. *Biophys. J.* **1992**, *63*, 1280–1285.

(11) Misra, V. K.; Hecht, J. L.; Sharp, K. A.; Friedman, R. A.; Honig, B. *J. Mol. Biol.* **1994**, *238*, 264–280.

region behaves like one of the charged groups on the polyion. The charge on the co-ion is renormalized by condensed counterions to the same extent as any of the charged groups on the polyion. A co-ion in the intermediate region behaves like a fractionally charged polyion group. The co-ion potential equals the negative of the counterion potential only in the Debye–Hückel-like far region. This situation destroys additivity. If a bipolar ion (which may be thought of as a counterion–co-ion pair) approaches a polyion, a strict additivity rule (overall potential equals isolated counterion potential plus isolated co-ion potential) is applicable only if the co-ion end of the bipolar ion is located in the far region.

Consider a bipolar ion located such that both of its ends are inside the near region. If the polyion is negatively charged, then the negative end of the bipolar ion may cooperate with the P charged groups on the polyion in the formation of a condensed layer of counterions. On the other hand, attached as it is to the positive end, the negative end is certainly distinct from a charged group on the polyion. Therefore, we use a renormalized charge $-(1 - \theta')q$ for the negative end of the bipolar ion, in contrast to the P renormalized charges $-(1 - \theta)q$ on the polyion. Here, θ and θ' are the fractional numbers of counterions condensed on each polyion charge and the negative end of the bipolar ion, respectively. For the polyion, θP makes sense as the total number of counterions shared by all the polyion charges in a condensed layer. An interpretation for the negative end of the bipolar ion would be that it is associated with a condensed counterion for the fraction of time θ' .

The free energy is set up along lines parallel to the development in ref 3. The number of counterions transferred from bulk concentration c to the condensed layer around the polyion or to the negative end of the bipolar ion is $P\theta + \theta'$. The interaction free energy between the negative end at r' and the polyion equals $2\xi(1 - \theta)(1 - \theta')K_0(\kappa r')$. The total free energy is minimized by setting its derivatives with respect to θ and θ' separately equal to zero. In the two resulting equations, the $\ln c$ terms are isolated and their coefficients are set equal to zero. The two equations resulting from this operation are

$$\xi(1 - \theta) - 1 = 0 \quad (22)$$

and

$$\xi(1 - \theta) - 1 - \frac{\xi}{P} + \frac{\xi(1 - \theta')}{P} = 0 \quad (23)$$

The solution of eq 22 is $\theta = 1 - (1/\xi)$, and when this value of θ is substituted into eq 23, it becomes clear that $\theta' = 0$. The

minimizing value of θ is familiar: $P(1 - \xi^{-1})$ is the total number of univalent counterions condensed on an isolated polyion with P charged groups. Intrusion of both ends of the overall neutral bipolar ion into the near region does not change the net charge density in this region, so there is no net release or gain of counterions on the polyion. Similarly, the negative end of the bipolar ion is unassociated with independent counterions, $\theta' = 0$, because the additional counterion required to condense into the near region in order to maintain the effective polyion charge density equal to the critical condensation value is automatically supplied by the positive end.

Since the number of counterions condensed on the negative end of the bipolar ion is zero in the far region, and, as we have just seen, in the near region as well, we may assume with some assurance that none are condensed on the negative end in the intermediate region. The physical reason would be that the negative end in the intermediate region would at most be required to condense some fraction of a counterion (in a time-average sense), and this requirement is overfulfilled by the unit charge forced to accompany the negative end as part of the covalent structure of the bipolar ion. In fact, we have verified that the intermediate region equations corresponding to eqs 22 and 23 have no solution in the physically meaningful range $0 \leq \theta' \leq 1$; free energy minimization at the boundary value $\theta' = 0$ is then the only plausible alternative. We generalize this rule to the collection of negative charged residues on a DNA-binding protein with net zero or positive charge: none of the negative protein charges are ion-paired with counterions. An additivity rule for the entire collection of protein charges, positive and negative, then follows if we set the potential for each negative charge equal to the potential for a positive charge but for a sign change.

The requirement $\theta' = 0$ (no ion-pairing of a negative protein charge with counterions) does not mean that $P\theta$, the number of counterions condensed on the DNA, is unaffected by the protein charges. For example, each positive protein charge located in the near region of DNA results in the release of one univalent counterion from the condensed layer. Similarly, each negative protein charge located in the near region of DNA would result in the addition of one counterion to the condensed layer (but this additional counterion is not ion-paired to the negative protein charge). If there are more positive protein charges in the near region than negative protein charges, there is a net release of counterions from the condensed layer. Protein charges positioned in the intermediate region, both positive and negative, also influence the value of $P\theta$.

JA9942437